

# Multimode Raman light-atom interface in warm atomic ensemble as multiple three-mode quantum operations

Michał Parniak<sup>a\*</sup>, Daniel Pęczak<sup>b</sup> and Wojciech Wasilewski<sup>a</sup>

<sup>a</sup>*Institute of Experimental Physics, Faculty of Physics, University of Warsaw, Pasteura 5, 02-093 Warsaw, Poland;* <sup>b</sup>*Institute of Physics, Polish Academy of Sciences, Al. Lotników 32/46, 02-668 Warsaw, Poland*

(Received 00 Month 20XX; final version received 00 Month 20XX)

We analyze the properties of a Raman quantum light-atom interface in long atomic ensemble and its applications as a quantum memory or two-mode squeezed state generator. We consider the weak-coupling regime and include both Stokes and anti-Stokes scattering and the effects of Doppler broadening in buffer gas assuming frequent velocity-averaging collisions. We find the Green functions describing multimode transformation from input to output fields of photons and atomic excitations. Proper mode basis is found via singular value decomposition for short interaction times. It reveals that triples of modes are coupled by a transformation equivalent to a combination of two beamsplitters and a two-mode squeezing operation. We analyze the possible transformations on an example of warm rubidium-87 vapor. The model we present bridges the gap between the Stokes only and anti-Stokes only interactions providing simple, universal description in a temporally and longitudinally multimode situation. Our results also provide an easy way to find an evolution of the states in a Schrödinger picture thus facilitating understanding and design.

**Keywords:** Quantum optics; Raman scattering; Quantum memory; Multimode interaction; Buffer gas; Warm atomic vapors; Light-atom interface

## 1. Introduction

The off-resonant Raman interface is a vividly developing approach to quantum memory [1, 2]. An off-resonant anti-Stokes scattering in optically thick atomic vapor can be used to transfer excitations from the optical field to atoms in the read-in process [3]. Atomic coherence that takes on the form of spinwave is created and can be converted back to light in the read-out process [4, 5]. The spinwaves can be stored and then further manipulated [6]. A similar approach incorporates cold atomic ensembles instead of warm vapors [7, 8]. The Raman process is perhaps the simplest out of many possible realizations of quantum memories. In addition, a Stokes transition can be driven by properly tuning the pump beam, which leads to the spontaneous creation of excitations pairs in the write-in process, where for each photon a single atom is excited in a spinwave [9]. The interface also lends itself to a multispatial mode use [10–12]. Simultaneous driving of both Stokes and anti-Stokes transitions leads to a number of interesting phenomena enabling quantum engineering [13–16]. When they are in perfect balance, quantum non-demolition (QND) measurement type of interaction occurs [17, 18].

Here we focus on the effects of coexistence of both Stokes and anti-Stokes scattering in the presence of Doppler broadening. We analyze the situation for a wide range of detunings resulting in rather arbitrary proportions between elementary processes. It turns out that in the off-resonant, high-optical-depth case when losses can be neglected the combined action of the Stokes and anti-

---

\*Corresponding author. Email: [michal.parniak@fuw.edu.pl](mailto:michal.parniak@fuw.edu.pl)

Stokes scattering creates similar spatiotemporal mode structure as each of them separately would [19, 20]. However, the transformation of the annihilation/creation operators of respective modes is more involved. It can be decomposed into a pair of beamsplitters and a squeezing operation between pairs of modes: atomic, photonic Stokes and photonic anti-Stokes. In particular we show that both read-out from atomic memory to light and read-in of light state into the memory typically involves significant squeezing of the quantum state. The squeezing can be only avoided when anti-Stokes coupling is much higher than the Stokes. The model we present facilitates understanding and design under realistic experimental conditions.

This paper is organized as follows. In Section 2 we write out equations of evolution of coupled quantum fields. We include effects of frequent collisions with buffer gas. The solution is given in a form of the input-output relations for which mode basis diagonalizing the relations exists. We analyze the quantum evolution of the coupled triples of modes. In Section 3 we rewrite the interaction of three fundamental modes in a form easiest to comprehend and analyze. Section 4 concludes the paper.

## 2. Evolution of fields

### 2.1. Maxwell-Bloch equations

We consider a spatially extended ensemble of length  $L$  of three or more level atoms moving with different velocities but otherwise identical. The atoms are assumed to have two long-lived ground levels  $|g\rangle$  and  $|h\rangle$  used to store quantum information. The Raman interaction is driven by intense classical field  $P$  in a square-shaped pulse of duration  $T$ . We consider only forward scattering and thus assume no dependence of the fields on perpendicular coordinates. We also neglect all kinds of decoherence which is justified for large optical depths. Initially all atoms are assumed to occupy  $|g\rangle$  level. As illustrated in Fig. 1(a) the interaction couples the atoms to weak quantum fields (sidebands)  $\hat{r}(z, t)$  and  $\hat{w}^\dagger(z, t)$ , corresponding to anti-Stokes and Stokes modes, respectively.

The beams are assumed to be virtually collinear and therefore only the velocity  $v$  of the atoms along the beams affects the interaction. The splitting of the ground levels is taken to be so small that the two-photon resonance condition is simultaneously met for all velocity classes. However the detuning of the pump  $P$  field from resonance is different for each velocity class and therefore the evolution of the atomic state is somewhat different. Thus we take the atomic coherence field operator  $\hat{b}(z, t, v)$ , understood within the Holstein-Primakoff approximation [21], to be velocity class dependent<sup>1</sup>.

Together with warm atomic ensembles an inert buffer gas, such as neon, krypton or xenon is used to make the motion of atoms diffusive and consequently prolong the lifetime of stored spatial mode [22, 23]. The presence of such buffer gas inherently leads to multiple effects affecting quantum memories [24], one of which are the velocity changing collisions. These collisions transfer atoms from velocity class  $v'$  into  $v$  with probability per unit time given by  $\gamma_v K(v \leftarrow v') dv'$ , where  $\gamma_v$  is the collision rate and  $K(v \leftarrow v')$  is the collisional kernel [25].

Under the assumption that the driving field  $P$  is off-resonant with given detuning from line centroid  $\Delta$ , the excited level can be adiabatically eliminated. The interaction between the atoms and the sidebands is given by a set of Maxwell-Bloch equations [26]. They can be cast in terms of field operators in a reference frame co-moving with weak light [20]:

$$\frac{\partial \hat{r}(z, t)}{\partial z} = \int \sqrt{g(v)} c_R(\Delta + kv) \hat{b}(z, t, v) dv \quad (1)$$

---

<sup>1</sup>The atomic field operator is normalized so that the commutator  $[\hat{b}(z, t, v), \hat{b}^\dagger(z', t, v')] = \delta(t-t')\delta(v-v')$ , therefore  $\hat{b}(z, t, v) = \frac{1}{\sqrt{N\Delta z \Delta v}} \sum_i |g_i\rangle \langle h_i|$ , where the summation runs through  $N$  atoms in slice  $\Delta z$  and velocity class  $\Delta v$ .

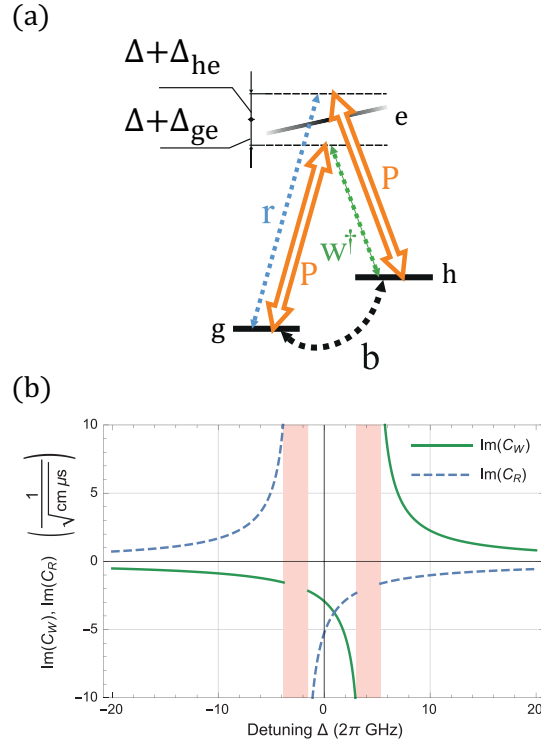


Figure 1. (color online) (a) Off-resonant Raman scattering in a 3-level atom. Linearly polarized pump of amplitude  $P$  couples two separate hyperfine components of the ground state,  $|g\rangle$  and  $|h\rangle$  via the excited state  $|e\rangle$ . Pump is detuned from the  $|g\rangle - |e\rangle$  transition by  $\Delta + \Delta_{ge}$  and from the  $|h\rangle - |e\rangle$  transition by  $\Delta + \Delta_{he}$ , where  $\Delta = 0$  means the pump is tuned to the line centroid. Tilting and shading of the upper level symbolizes the Doppler shift and atomic population distribution respectively. (b) Imaginary parts of coherent scattering coefficients  $c_R(\Delta)$ ,  $c_W(\Delta)$  for rubidium 87 D1 line ( $\lambda \approx 795$  nm) as a function of detuning  $\Delta$  between the driving field and the centroid of the line. We take two hyperfine components of the ground state as levels  $|g\rangle = |F = 1, m_F = 0\rangle$  and  $|h\rangle = |F = 2, m_F = 0\rangle$ . We take the atom number density equal  $N = 10^{12}$  cm $^{-3}$  and pump field Rabi frequency equal to the natural linewidth  $\Gamma/2\pi = 5.75$  MHz. Real parts of the coherent scattering coefficients are found to be much smaller than the plotted imaginary parts and consequently we exclude them from consideration. Shaded regions close to resonances (closer than three times the Doppler width) where losses and pump absorption have significant effect are excluded from the analysis.

$$\frac{\partial \hat{w}^\dagger(z, t)}{\partial z} = \int \sqrt{g(v)} c_W(\Delta + kv) \hat{b}(z, t, v) dv \quad (2)$$

$$\begin{aligned} \frac{\partial \hat{b}(z, t, v)}{\partial t} &= \sqrt{g(v)} c_W^*(\Delta + kv) \hat{w}^\dagger(z, t) \\ &+ \sqrt{g(v)} c_R(\Delta + kv) \hat{r}(z, t) - s(\Delta + kv) \hat{b}(z, t, v) \\ &+ \gamma_v \int K(v \leftarrow v') \sqrt{\frac{g(v')}{g(v)}} \hat{b}(z, t, v') dv', \end{aligned} \quad (3)$$

where  $g(v) = \frac{1}{\sqrt{2\pi\sigma^2}} \exp(-\frac{v^2}{2\sigma^2})$  is the thermal velocity distribution and  $k = \frac{2\pi}{\lambda}$  is the light wavevector. The interaction is parametrized by coherent scattering coefficients  $c_R(\Delta)$  and  $c_W(\Delta)$  plotted in Fig. 1(b) and given by:

$$c_R(\Delta) = -\sqrt{\frac{N\omega}{2\hbar c\epsilon_0}} \sum_e \frac{P d_{ge} d_{eh}}{(\Gamma - 2i(\Delta + \Delta_{he}))\hbar} \quad (4)$$

$$c_W(\Delta) = -\sqrt{\frac{N\omega}{2\hbar c\epsilon_0}} \sum_e \frac{P d_{he} d_{eg}}{(\Gamma + 2i(\Delta + \Delta_{ge}))\hbar} \quad (5)$$

where  $\omega = \frac{2\pi c}{\lambda}$ ,  $\Delta_{ij}$  is the difference between resonant frequency of  $|i\rangle - |j\rangle$  transition and line central frequency (also see Fig. 1(a) for reference),  $d_{ij}$  is the dipole moment for this transition and physical constants are denoted as usual. The sum runs through all possible excited states  $|e\rangle$ . Limiting cases correspond to  $|c_W| \ll |c_R|$  for anti-Stokes scattering and  $|c_R| \ll |c_W|$  for Stokes scattering. If the pump is far-detuned, so that  $\Delta + \Delta_{ij} \gg \Gamma$ , we find the imaginary parts of coherent scattering coefficients  $c_R$  and  $c_W$  to be strongly dominant over the real parts, under the assumption that pump amplitude  $P$  is real. Indeed, the classical field amplitude  $P$  can be always made real by suitable shift of the time reference. The same assumptions hold for the differential Stokes shift  $s(\Delta)$  given by:

$$s(\Delta) = \sum_e \frac{|P d_{eh}|^2}{2(\Gamma - 2i(\Delta + \Delta_{he}))\hbar^2} + \frac{|P d_{eg}|^2}{2(\Gamma + 2i(\Delta + \Delta_{ge}))\hbar^2}. \quad (6)$$

## 2.2. Fast collisions approximation

The inclusion of velocity changing collision kernel in Eq. (3) may severely influence the solution, as different Maxwellian velocity distribution preserving kernels might be used [25, 27, 28]. However, if we assume that the collisions are fast compared to the Raman interaction  $\gamma_v \gg Lc_{R,W}^2$ , then the velocity dependence of number operator of atoms in  $|h\rangle$  state represented by  $\hat{b}^\dagger(z, t, v)\hat{b}(z, t, v)$  remains close to thermal equilibrium. Consequently, we may separate out the known, Gaussian velocity dependence and assume  $\hat{b}(z, t, v) = \hat{b}(z, t)\sqrt{g(v)}$ .

The equation (3) for  $\hat{b}(z, t, v)$  can now be integrated formally and averaged over velocity distribution  $\hat{b}(z, t) = \int \sqrt{g(v)}\hat{b}(z, t, v)dv$ , yielding:

$$\hat{b}(z, t) = \hat{b}(z, 0) + \int_0^t e^{-(t-t')\bar{s}} \left( \bar{c}_R \hat{r}(z, t') + \bar{c}_W^* \hat{w}^\dagger(z, t') \right) dt', \quad (7)$$

where the differential Stokes shift  $s(\Delta)$  and coherent scattering coefficients  $c_R(\Delta)$  and  $c_W(\Delta)$  are now averaged according to the formula  $\bar{x} = \int x(\Delta + kv)g(v)dv$ . Substituting this result to Eqs. (1)–(2) gives the following equation of evolution for the photonic modes:

$$\begin{aligned} \frac{\partial}{\partial z} \begin{pmatrix} \hat{r}(z, t) \\ \hat{w}^\dagger(z, t) \end{pmatrix} &= \begin{pmatrix} \bar{c}_R \\ \bar{c}_W \end{pmatrix} \hat{b}(z, 0) e^{-\bar{s}t} \\ + \int_0^t e^{-(t-t')\bar{s}} &\begin{pmatrix} \bar{c}_R^2 & \bar{c}_R \bar{c}_W^* \\ \bar{c}_W \bar{c}_R & |\bar{c}_W|^2 \end{pmatrix} \begin{pmatrix} \hat{r}(z, t') \\ \hat{w}^\dagger(z, t') \end{pmatrix} dt'. \end{aligned} \quad (8)$$

Note the average atomic coefficients  $\bar{c}_W$ ,  $\bar{c}_R$  and  $\bar{s}$  are virtually purely imaginary for far-detuned pump field. From now on we will assume these coefficients are imaginary.

### 2.3. Input-output relations

The solution of equations (7)–(8) takes on a form of a linear transformation between the input and output quantum fields. First, a squeezing transformation i.e. hyperbolic rotation  $R(\zeta)$  between the photonic modes is used to diagonalize the matrix from Eq. (8). Modes  $\hat{c}^\dagger(z, t)$  and  $\hat{d}(z, t)$  are defined as linear combinations of  $\hat{r}(z, t)$  and  $\hat{w}^\dagger(z, t)$  according to the formulas:

$$\begin{pmatrix} \hat{r}(L, t) \\ \hat{w}^\dagger(L, t) \end{pmatrix} = R^{-1}(\zeta) \begin{pmatrix} \hat{c}^\dagger(L, t) \\ \hat{d}(L, t) \end{pmatrix} \quad (9)$$

$$\begin{pmatrix} \hat{c}^\dagger(0, t) \\ \hat{d}(0, t) \end{pmatrix} = R(\zeta) \begin{pmatrix} \hat{r}(0, t) \\ \hat{w}^\dagger(0, t) \end{pmatrix} \quad (10)$$

where the diagonalizing hyperbolic rotation matrix is defined as

$$R(\zeta) = \begin{cases} \begin{pmatrix} \sinh(\zeta) & \cosh(\zeta) \\ \cosh(\zeta) & \sinh(\zeta) \end{pmatrix} & \begin{array}{l} \text{with } \zeta = \text{atanh} \left| \frac{\bar{c}_R}{\bar{c}_W} \right| \\ \text{for } |\bar{c}_W| > |\bar{c}_R| \end{array} \\ \begin{pmatrix} \cosh(\zeta) & \sinh(\zeta) \\ \sinh(\zeta) & \cosh(\zeta) \end{pmatrix} & \begin{array}{l} \text{with } \zeta = \text{atanh} \left| \frac{\bar{c}_W}{\bar{c}_R} \right| \\ \text{for } |\bar{c}_W| < |\bar{c}_R| \end{array} \end{cases} \quad (11)$$

Note a significant difference between the two cases from above equation. When  $|\bar{c}_W| > |\bar{c}_R|$  both  $\hat{c}(z, t)$  and  $\hat{d}(z, t)$  are annihilation operators. On the contrary when  $|\bar{c}_W| < |\bar{c}_R|$  both  $\hat{c}(z, t)$  and  $\hat{d}(z, t)$  play role of bosonic creation operators. We can generally write  $[\hat{c}(z, t), \hat{c}^\dagger(z, t')] = [\hat{d}(z, t), \hat{d}^\dagger(z, t')] = \text{sgn}(|\bar{c}_W| - |\bar{c}_R|)\delta(t - t')$ . In particular in the limiting cases of pure Stokes or pure anti-Stokes scattering corresponding to  $|\bar{c}_W| \gg |\bar{c}_R|$  and  $|\bar{c}_W| \ll |\bar{c}_R|$ , the  $R(\zeta)$  is an identity or mode-swap transformation, respectively.

The mode  $\hat{d}(z, t)$  turns out to be decoupled and constant, thus  $\hat{d}(L, t) = \hat{d}(0, t)$ . The equations coupling atoms  $\hat{b}(z, t)$  with photonic mode  $\hat{c}(z, t)$  are the same as in single-sideband Raman scattering [20, 26, 29] and their solution reads:

$$\begin{aligned} \hat{b}(z, T) &= \int_0^T \hat{c}^\dagger(0, t') \sqrt{\kappa} \Sigma_0(z, T - t') dt' \\ + \int_0^z \hat{b}(z', 0) &[e^{-T\bar{s}} \delta(z - z') + T \Sigma_1(z - z', T)] dz' \end{aligned} \quad (12)$$

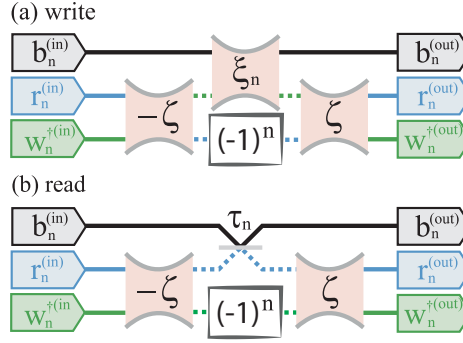


Figure 2. (color online) Decompositions of interaction between  $n$ -th coupled triple of modes into hyperbolic rotations  $R(\zeta)$  and squeezing by  $\exp(\xi_n)$  or beamsplitter with transmission  $\tau_n$ . (a) Stokes domination  $|\bar{c}_W| > |\bar{c}_R|$  [corresponding matrix decomposition given by Eq. (16)] and (b) anti-Stokes domination  $|\bar{c}_W| < |\bar{c}_R|$  [corresponding matrix decomposition given by Eq. (17)].

$$\begin{aligned} \hat{c}^\dagger(L, t) &= \int_0^L \hat{b}(z', 0) \sqrt{\kappa} \Sigma_0(L - z', t) dz' \\ &+ \int_0^t \hat{c}^\dagger(0, t') [L \Sigma_1(L, t - t') + \delta(t - t')] dt' \end{aligned} \quad (13)$$

where the interaction strength is measured by

$$\kappa = \bar{c}_R^2 + |\bar{c}_W|^2 \quad (14)$$

and  $\Sigma_1(z, t) = \sqrt{\frac{\kappa}{zt}} I_1(2\sqrt{\kappa zt})$ ,  $\Sigma_0(z, t) = I_0(2\sqrt{\kappa zt})$ , where  $I_n(x)$  are the modified Bessel functions of the first kind.

#### 2.4. Singular modes

The input-output relations in Eqs. (12) and (13) can be simplified by suitable choice of mode basis for atomic  $u_n^{(in/out)}(z)$  and photonic  $v_n^{(in/out)}(t)$  fields in which  $n$ -th atomic mode mixes only with photonic modes with the same number [11, 19, 20]. The annihilation operators for modes before and after the interaction are defined as follows:  $\hat{b}_n^{(in)} = \int u_n^{(in)}(z) \hat{b}(z, 0) dz$ ,  $\hat{r}_n^{(in)} = \int v_n^{(in)}(t) \hat{r}(0, t) dt$ ,  $\hat{w}_n^{\dagger(in)} = \int v_n^{(in)}(t) \hat{w}^\dagger(0, t) dt$ ,  $\hat{b}_n^{(out)} = \int u_n^{(out)}(z) \hat{b}(z, T) dz$ ,  $\hat{r}_n^{(out)} = \int v_n^{(out)}(t) \hat{r}(L, t) dt$  and  $\hat{w}_n^{\dagger(out)} = \int v_n^{(out)}(t) \hat{w}^\dagger(L, t) dt$ . The resulting operator, e.g.  $\hat{b}_n^{(in)}$ , annihilates a single excitation in the respectful mode, in this case spatial mode  $u_n^{(in)}(z)$ . The modes are orthonormal and the commutator  $[\hat{b}_m^{(in)}, \hat{b}_n^{(in)\dagger}] = \delta_{mn}$  and the same holds for all other operators. Then the relations between  $n$ -th input and output operators are given by a  $3 \times 3$  matrix  $\mathbf{G}_n$  of real values equivalent to a diagram given in Fig. 2:

$$\begin{pmatrix} \hat{b}_n^{(out)} \\ \hat{r}_n^{(out)} \\ \hat{w}_n^{(out)\dagger} \end{pmatrix} = \mathbf{G}_n \begin{pmatrix} \hat{b}_n^{(in)} \\ \hat{r}_n^{(in)} \\ \hat{w}_n^{(in)\dagger} \end{pmatrix} \quad (15)$$

If  $|\bar{c}_W| > |\bar{c}_R|$ , the centerpiece is a squeezing operation, as in Fig. 2(a):

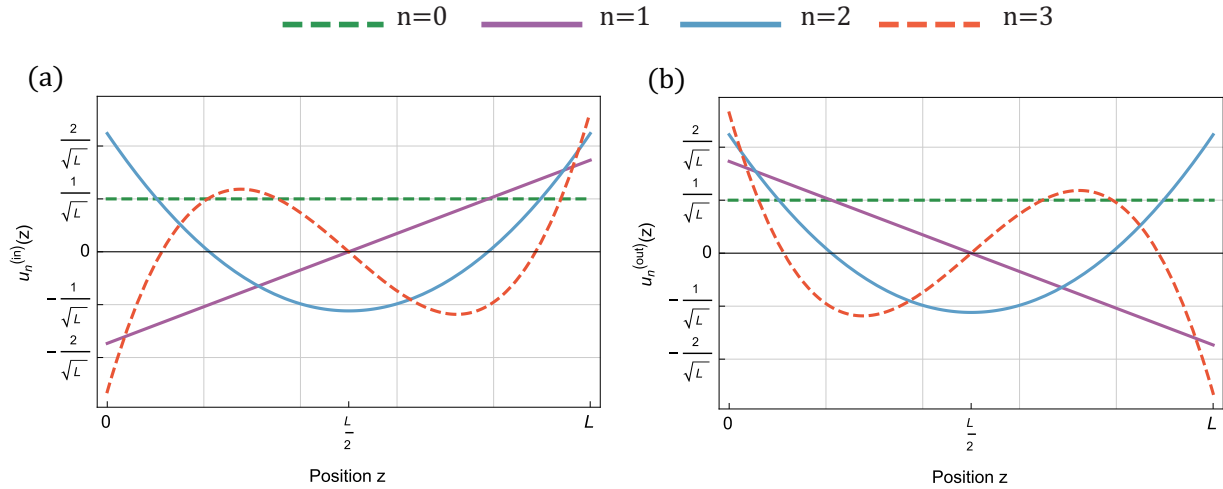


Figure 3. (color online) Atomic (a) input  $u_n^{in}(z)$  and (b) output  $u_n^{out}(z)$  mode functions for first four coupled modes, including the flat fundamental mode ( $n = 0$ ).

$$\mathbf{G}_n = (1 \oplus R(\zeta)) \left[ \begin{pmatrix} \cosh(\xi_n) & \sinh(\xi_n) \\ \sinh(\xi_n) & \cosh(\xi_n) \end{pmatrix} \oplus (-1)^n \right] (1 \oplus R^{-1}(\zeta)) \quad (16)$$

When  $|\bar{c}_W| < |\bar{c}_R|$ , squeezing is replaced by a beamsplitter as depicted in Fig. 2(b):

$$\mathbf{G}_n = (1 \oplus R(\zeta)) \left[ \begin{pmatrix} \sqrt{1 - \tau_n^2} & \tau_n \\ -\tau_n & \sqrt{1 - \tau_n^2} \end{pmatrix} \oplus (-1)^n \right] (1 \oplus R^{-1}(\zeta)) \quad (17)$$

The mode basis for atomic  $u_n^{(in/out)}(z)$  and photonic fields  $v_n^{(in/out)}(t)$  as well as squeezing  $\xi_n$  or beamsplitter transmission  $\tau_n$  for the central operation are calculated from singular value decomposition of Green functions from Eqs. (12) and (13) [11, 19, 20]. Normalized to length of the atomic sample  $L$  and pump pulse duration  $T$  they depend solely on the product  $\kappa LT = (\bar{c}_R^2 + |\bar{c}_W|^2)LT$ . For weak interaction we calculate squeezing  $\xi_n = (\kappa LT)^{n+1/2}$  if  $|\bar{c}_W| > |\bar{c}_R|$  or beamsplitter transmission  $\tau_n = (-\kappa LT)^{n+1/2}$  if  $|\bar{c}_W| < |\bar{c}_R|$ . The mode functions are in the lowest order independent of  $\kappa$ :  $u_n^{(in)}(z) = \frac{1}{\sqrt{L(2n+1)}} P_n(2z/L - 1)$ ,  $u_n^{(out)}(z) = \frac{1}{\sqrt{L(2n+1)}} P_n(1 - 2z/L)$ ,  $v_n^{(in)}(z) = \frac{1}{\sqrt{T(2n+1)}} P_n(2t/T - 1)$ ,  $v_n^{(out)}(t) = \frac{1}{\sqrt{T(2n+1)}} P_n(1 - 2t/T)$  where  $P_n(x)$  is  $n$ -th Legendre polynomial. We plot exemplary input and output atomic mode functions in Fig. 3.

Note that in the limiting cases of pure Stokes or pure anti-Stokes scattering corresponding to  $|\bar{c}_W| \gg |\bar{c}_R|$  and  $|\bar{c}_W| \ll |\bar{c}_R|$  we recover either two-mode squeezing of  $\hat{b}_n$  with  $\hat{w}_n^\dagger$  or a beamsplitter transformation between  $\hat{b}_n$  and  $\hat{r}_n$ .

### 3. Results

#### 3.1. Parameters and circuit diagram

Now we proceed with detailed interpretation of total transformation for any mode triple. Here and in the following we drop index  $n$  and consider only the most coupled mode  $n = 0$ . In the previous section we have shown the interaction of three coupled modes can be represented by squeezing or

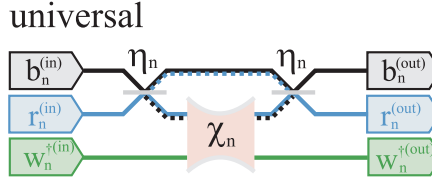


Figure 4. (color online) Universal decomposition of Raman interaction for  $n$ -th coupled triple atomic  $\hat{b}_n$ , photonic Stokes  $\hat{w}_n$  and anti-Stokes  $\hat{r}_n$  modes in terms of beamsplitters of transmission  $\eta_n$  and central squeezing by  $\exp(\chi_n)$ . Those parameters depend on both detuning from respective atomic resonances  $\Delta$  and resulting ratio of the Stokes to anti-Stokes coupling  $\bar{c}_W/\bar{c}_R$  as well as the optical depth and duration of the interaction. Achievable range of parameters are plotted in Fig. 5. For simplification, in text parameters are given for  $n = 0$  without index.

beamsplitter transformation sandwiched between hyperbolic rotations as depicted in Fig. 2. The hyperbolic rotation can be interpreted as another squeezing therefore we effectively describe the interaction as a composition of squeezing operations, which makes total transformation  $\mathbf{G}$  difficult to tackle.

To facilitate understanding and design we decompose the total transformation  $\mathbf{G}$  as a squeezing sandwiched in between beamsplitters depicted in Fig. 4. This form is valid for any values of  $\bar{c}_W$  and  $\bar{c}_R$  and corresponds to the following product:

$$\mathbf{G} = (B(\eta) \oplus 1)(1 \oplus S(\chi))(B(\eta) \oplus 1) \quad (18)$$

where  $B(\eta) = \begin{pmatrix} \sqrt{1-\eta^2} & \eta \\ -\eta & \sqrt{1-\eta^2} \end{pmatrix}$  is the beamsplitter transformation between the atomic mode and anti-Stokes mode with transmission  $\eta$ , and  $S(\chi) = \begin{pmatrix} \cosh(\chi) & \sinh(\chi) \\ \sinh(\chi) & \cosh(\chi) \end{pmatrix}$  is the squeezing operation.

The relation between parameters depicted in Fig. 2 i.e. hyperbolic rotation  $\zeta$  and squeezing  $\xi$  or transmission  $\tau$  and parameters of general transformation is found in a closed form. For the squeezing parameter  $\chi$  we obtain:

$$\cosh(\chi) = \begin{cases} \cosh^2(\zeta) \cosh(\xi) - \sinh^2(\zeta) & \text{for } |\bar{c}_W| > |\bar{c}_R| \\ \cosh^2(\zeta) - \sqrt{1-\tau^2} \sinh^2(\zeta) & \text{for } |\bar{c}_W| < |\bar{c}_R| \end{cases} \quad (19)$$

and for the beamsplitter transmission  $\eta$ :

$$\eta = \begin{cases} \sqrt{\frac{1+\cosh(\xi)}{1+\cosh(\chi)}} & \text{for } |\bar{c}_W| > |\bar{c}_R| \\ \sqrt{\frac{1+\sqrt{1-\tau^2}}{1+\cosh(\chi)}} & \text{for } |\bar{c}_W| < |\bar{c}_R| \end{cases} \quad (20)$$

In Fig. 5 we plot the squeezing  $\chi$  and beamsplitter transmission  $\eta$  as a function of pump detuning  $\Delta$  which determines hyperbolic rotation  $\zeta$  for various interaction strengths. We observe that not all transformations are achievable. An ideal readout process corresponds to using 50/50 beamsplitter i.e.  $\eta = 1/\sqrt{2}$  twice without squeezing ( $\chi = 0$ ). At opposite extreme, spontaneous pair creation process corresponds to transparent beamsplitters  $\eta = 1$  around squeezing  $\chi$  in the first order equal  $\sqrt{\kappa LT}$ . We see that neither is actually possible within the realistic model we present. To get as close as possible to pure Stokes or anti-Stokes process we need to tune the pump close to appropriate resonant transition, so that either  $|\bar{c}_W| \gg |\bar{c}_R|$  or  $|\bar{c}_R| \gg |\bar{c}_W|$ .



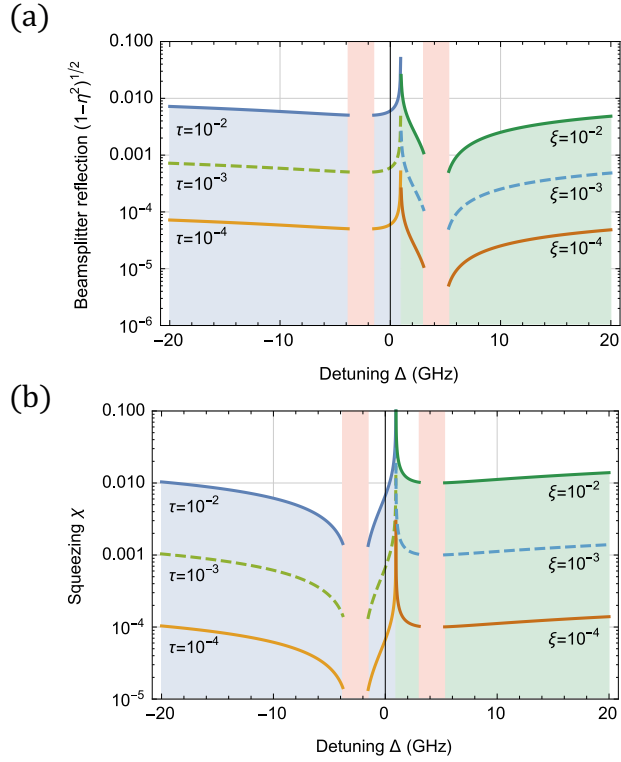


Figure 5. (color online) (a) Transmission of beamsplitter  $\eta$  and (b) squeezing  $\chi$  in the universal decomposition depicted in Fig. 4 and described by Eq. (18) as a function of pump detuning  $\Delta$  for a various interaction parameters from decomposition depicted in Fig. 2: squeezing  $\xi$  for domination of the Stokes  $|\bar{c}_W| > |\bar{c}_R|$  or transmission  $\tau$  for domination of the anti-Stokes  $|\bar{c}_R| > |\bar{c}_W|$ .

### 3.2. Output states

In this section we study the output states of quantum memory or squeezed state generator in typical experimental situation. First, we consider the process of spontaneous Raman scattering, ideally realizing two-mode squeezing. The initial state of  $n$ -th mode is  $|000\rangle_{\text{in}}$  regardless of mode index  $n$ , and  $|\bar{c}_W| > |\bar{c}_R|$ . The ket  $|k, l, m\rangle_{\text{in/out}}$  denotes  $k$  excitations in atomic spinwave mode  $u_n^{(\text{in/out})}(z)$ ,  $l$  photons in the anti-Stokes mode  $v_n^{(\text{in/out})}(t)$  and  $m$  photons in the Stokes mode  $v_n^{(\text{in/out})}(t)$ . From the universal decomposition depicted in Fig. 4 we can easily obtain the output state  $\mathcal{U}_n|000\rangle_{\text{in}}$  in the Schrödinger picture with  $\mathcal{U}_n$  being the evolution operator. The output is most populated for  $n = 0$  to which we limit ourselves dropping the index  $n$  in the following consideration. The final state is a two-mode squeezed  $\exp(\chi)$  times state with one mode transmitted through a beamsplitter of transmission  $\eta$ :

$$\begin{aligned} \mathcal{U}|000\rangle_{\text{in}} &= \frac{1}{\cosh(\chi)} \sum_{j=0}^{\infty} \tanh^j(\chi) \\ &\times \sum_{k=0}^j \sqrt{\binom{j}{k}} (1-\eta^2)^{k/2} \eta^{j-k} |j-k, k, j\rangle_{\text{out}} \end{aligned} \quad (21)$$

Note, that the above equation is valid for  $|\bar{c}_W| < |\bar{c}_R|$  as well. As squeezing  $\xi = \sqrt{(\bar{c}_R^2 + |\bar{c}_W|^2)LT}$

is small, we may obtain the following (unnormalized) expansion:

$$\begin{aligned} \mathcal{U}|000\rangle_{\text{in}} &\approx |000\rangle_{\text{out}} + \cosh(\zeta)|101\rangle_{\text{out}}\xi \\ &+ (\cosh^2(\zeta)|202\rangle_{\text{out}} + \cosh(\zeta)\sinh(\zeta)|011\rangle_{\text{out}})\xi^2 + \dots \end{aligned} \quad (22)$$

We observe that in the first order of interaction we indeed create a pair of photon and an atomic excitation, which is a perfect write-in process. In the second order we not only create two such pairs, but also a pair of photons with each of the photons in one of the photonic modes, corresponding to spontaneous four-wave-mixing process with degenerate pump. Note, that the heralding of two-atom excitation can be made by counting the photons only in the Stokes sideband. This is possible by spectral filtering indeed necessary in many experiments [5, 10, 13].

Main quantum memory operation modes are read-in, that is mapping single photon in anti-Stokes mode to atomic mode, and the opposite read-out operation [3]. Transforming the operators according to the known  $\mathbf{G}$  transformation, for  $\tau \ll 1$  we can express the output state in the following way:

$$\begin{aligned} &\mathcal{U}|010\rangle_{\text{in}} \\ &= (-\tau \cosh(\zeta)\hat{b}^\dagger + (1 - \frac{\tau^2}{2} \cosh^2(\zeta))\hat{r}^\dagger + \frac{\tau^2}{2} \cosh(\zeta)\sinh(\zeta)\hat{w})\mathcal{U}|000\rangle_{\text{in}} \end{aligned} \quad (23)$$

Where the operators  $\hat{b}^\dagger$ ,  $\hat{r}^\dagger$  and  $\hat{w}$  are bosonic creation/annihilation operators in Schrödinger picture acting on kets  $|k, l, m\rangle$  in the usual way, and we calculate  $\mathcal{U}|000\rangle_{\text{in}}$  from Eq. (21). We obtain the following expansion for the unnormalized state:

$$\mathcal{U}|010\rangle_{\text{in}} \approx |010\rangle_{\text{out}} + (\cosh(\zeta)|100\rangle_{\text{out}} + \sinh(\zeta)|111\rangle_{\text{out}})\tau \quad (24)$$

As expected, no state transfer occurs in the zeroth order. In the first order photon is transferred to the memory, but also a pair of Stokes photon and an atomic excitation is created. Note that in typical experimental situations  $\tau$  is close to unity for many modes. In this regime contribution of Stokes photons might be even more significant. Very similarly, when the quantum memory contains a single excitation, we may calculate how the state is transformed during read-out. For small  $\tau$  the transformation is following:

$$\begin{aligned} &\mathcal{U}|010\rangle_{\text{in}} \\ &= ((1 - \tau^2/2)\hat{b}^\dagger + \tau \cosh(\zeta)\hat{r}^\dagger - \tau \sinh(\zeta)\hat{w})\mathcal{U}|000\rangle_{\text{in}} \end{aligned} \quad (25)$$

The output state can be expanded again, to show that in the first order pair of photons and atomic excitations are created as well:

$$\mathcal{U}|100\rangle_{\text{in}} \approx |100\rangle_{\text{out}} + (-\cosh(\zeta)|010\rangle_{\text{out}} + \sqrt{\cosh(2\zeta) - 1}|201\rangle_{\text{out}})\tau \quad (26)$$

The above calculations show that spectral filtering is extremely important, as output state will always be polluted by spontaneously created photons even in the lowest order for weak interaction. Finally, we note that the ratio of the Stokes to anti-Stokes coupling  $\bar{c}_W/\bar{c}_R$  depends solely on parameters of atoms. This ratio should be minimized [30, 31] to ensure more faithful memory operation, as less spontaneous Stokes photons will be emitted.

## 4. Conclusions

We have introduced a model that allows us to describe Raman interaction with both Stokes and anti-Stokes sideband present in a long atomic sample in the presence of Doppler broadening under the weak interaction regime. As an exemplary medium we take warm rubidium 87 vapors contained in an inert buffer gas. The gas makes the motion of the atoms diffusive, allowing longer memory lifetime, and induces fast velocity-class thermalization, which we take into account in our model. Within this regime we are able to use singular value decomposition [11, 19, 20, 32] to find modes of the interaction. In this special mode bases for the field of atomic excitations, Stokes and anti-Stokes photons only triples of modes are coupled, one from each of the fields. We find closed expressions for the mode functions and coupling strengths in the weak coupling regime.

The interaction between any triple of modes constituting Raman interface is easiest understood when further decomposed into a product of three two-mode quantum operations, as depicted in Fig. 4. We give closed expressions for the parameters of constituent operations. We analyzed which transformations are achievable in case of warm rubidium 87 vapors.

Neither pure Stokes nor pure anti-Stokes scattering is possible, as one process is always accompanied by another. The effects of this interplay are easily analyzed within the framework developed. As an example we discuss effects on the storage in and retrieval from the quantum memory. Mapping ideal single excitation is inevitably accompanied by creation of additional excitations due to four-wave mixing even when interaction is weak. These processes can be suppressed by minimizing the ratio of the Stokes to anti-Stokes coupling which is possible in atomic vapors to a limited extent [30, 31].

We believe that our results may serve as a zeroth-order approximation for modeling various deleterious effects leading to decoherence such as absorption, spontaneous emission and effects due to motion of atoms. Multimode decoherence typically leads to quite complex results [33]. Finally we observe that the presented model may be applied to many similar systems, where exact atomic structure is different [2, 34–37].

## Acknowledgments

We acknowledge insightful discussions with M. Dąbrowski and M. Jachura, as well as generous support of K. Banaszek.

## Funding

This work was supported by the National Science Center (Poland) Grant No. DEC-2011/03/D/ST2/01941 and by the Polish Ministry of Science and Higher Education “Diamantowy Grant” Project No. DI2013 011943.

## References

- [1] Reim, K.F.; Michelberger, P.; Lee, K.C.; Nunn, J.; Langford, N.K.; et al. *Phys. Rev. Lett.* **2011**, *107* (5), 053603.
- [2] Heshami, K.; Santori, C.; Khanaliloo, B.; Healey, C.; Acosta, V.M.; Barclay, P.E.; et al. *Phys. Rev. A* **2014**, *89* (4), 040301.
- [3] Michelberger, P.S.; Champion, T.F.M.; Sprague, M.R.; Kaczmarek, K.T.; Barbieri, M.; Jin, X.M.; England, D.G.; Kolthammer, W.S.; Saunders, D.J.; Nunn, J.; et al. *New J. Phys.* **2015**, *17* (4), 043006.
- [4] van der Wal, C.H.; Eisaman, M.D.; André, A.; Walsworth, R.L.; Phillips, D.F.; Zibrov, A.S.; et al. *Science* **2003**, *301* (5630), 196–200.

- [5] Bashkansky, M.; Fatemi, F.K.; Vurgaftman, I. *Opt. Lett.* **2012**, *37* (2), 142–4.
- [6] Hosseini, M.; Sparkes, B.M.; Hétet, G.; Longdell, J.J.; Lam, P.K.; et al. *Nature* **2009**, *461* (7261), 241–5.
- [7] Bimbard, E.; Boddeda, R.; Vitrant, N.; Grankin, A.; Parigi, V.; Stanojevic, J.; Ourjountsev, A.; et al. *Phys. Rev. Lett.* **2014**, *112* (3), 033601.
- [8] Ding, D.S.; Zhang, W.; Zhou, Z.Y.; Shi, S.; Shi, B.S.; et al. *Nature Photon.* **2015**, *9* (5), 332–338.
- [9] Duan, L.M.; Lukin, M.D.; Cirac, J.I.; et al. *Nature* **2001**, *414* (6862), 413–8.
- [10] Chrapkiewicz, R.; Wasilewski, W. *Opt. Express* **2012**, *20* (28), 29540.
- [11] Kołodziej, J.; Chwedeńczuk, J.; Wasilewski, W. *Phys. Rev. A* **2012**, *86* (1), 013818.
- [12] Higginbottom, D.B.; Sparkes, B.M.; Rancic, M.; Pinel, O.; Hosseini, M.; Lam, P.K.; et al. *Phys. Rev. A* **2012**, *86* (2), 023801.
- [13] Dąbrowski, M.; Chrapkiewicz, R.; Wasilewski, W. *Opt. Express* **2014**, *22* (21), 26076.
- [14] de Echaniz, S.R.; Koschorreck, M.; Napolitano, M.; Kubasik, M.; et al. *Phys. Rev. A* **2008**, *77* (3), 032316.
- [15] Brannan, T.; Qin, Z.; MacRae, A.; et al. *Opt. Lett.* **2014**, *39* (18), 5447–5450.
- [16] Wu, C.; Raymer, M.G.; Wang, Y.Y.; et al. *Phys. Rev. A* **2010**, *82* (5), 053834.
- [17] Wasilewski, W.; Fernholz, T.; Jensen, K.; Madsen, L.S.; Krauter, H.; Muschik, C.; et al. *Opt. Express* **2009**, *17* (16), 14444.
- [18] Sewell, R.J.; Napolitano, M.; Behbood, N.; Colangelo, G.; et al. *Nature Photon.* **2013**, *7* (7), 517–520.
- [19] Wasilewski, W.; Raymer, M.G. *Phys. Rev. A* **2006**, *73* (6), 063816.
- [20] Raymer, M.G. *J. Mod. Opt.* **2004**, *51* (12), 1739–1759.
- [21] Holstein, T.; Primakoff, H. *Phys. Rev.* **1940**, *58* (12), 1098–1113.
- [22] Parniak, M.; Wasilewski, W. *Appl. Phys. B* **2014**, *116* (2), 415–421.
- [23] Chrapkiewicz, R.; Wasilewski, W.; Radzewicz, C. *Opt. Commun.* **2014**, *317*, 1–6.
- [24] Manz, S.; Fernholz, T.; Schmiedmayer, J.; et al. *Phys. Rev. A* **2007**, *75* (4), 040101.
- [25] McGuyer, B.H.; Marsland III, R.; Olsen, B.A.; et al. *Phys. Rev. Lett.* **2012**, *108* (18), 183202.
- [26] Raymer, M.G.; Mostowski, J. *Phys. Rev. A* **1981**, *24* (4), 1980–1993.
- [27] Marsland III, R.; McGuyer, B.H.; Olsen, B.A.; et al. *Phys. Rev. A* **2012**, *86* (2), 023404.
- [28] Kryszewski, S.; Gondek, J. *Phys. Rev. A* **1997**, *56* (5), 3923–3936.
- [29] Raymer, M.G.; Walmsley, I.A.; Mostowski, J.; et al. *Phys. Rev. A* **1985**, *32* (1), 332–344.
- [30] Vurgaftman, I.; Bashkansky, M. *Phys. Rev. A* **2013**, *87* (6), 063836.
- [31] Zhang, K.; Guo, J.; Chen, L.Q.; Yuan, C.; Ou, Z.Y.; et al. *Phys. Rev. A* **2014**, *90* (3), 033823.
- [32] Gerke, S.; Sperling, J.; Vogel, W.; Cai, Y.; Roslund, J.; Treps, N.; et al. *Phys. Rev. Lett.* **2015**, *114* (5), 050501.
- [33] Chrapkiewicz, R.; Wasilewski, W. *J. Mod. Opt.* **2010**, *57* (5), 345–355.
- [34] Parniak, M.; Wasilewski, W. *Phys. Rev. A* **2015**, *91* (2), 023418.
- [35] Bustard, P.J.; Erskine, J.; England, D.G.; Nunn, J.; Hockett, P.; Lausten, R.; Spanner, M.; et al. *Opt. Lett.* **2015**, *40* (6), 922–5.
- [36] Rieländer, D.; Kuhluer, K.; Ledingham, P.M.; Gündoğan, M.; Fekete, J.; Mazzera, M.; et al. *Phys. Rev. Lett.* **2014**, *112* (4), 040504.
- [37] Ding, D.S.; Jiang, Y.K.; Zhang, W.; Zhou, Z.Y.; Shi, B.S.; et al. *Phys. Rev. Lett.* **2015**, *114* (9), 093601.